EJN fens European Journal of Neuroscience

European Journal of Neuroscience, Vol. 30, pp. 242–250, 2009 doi:10.1111/j.1460-9568.2009.06812.x

NEUROSYSTEMS

Dose-dependent effect of isoflurane on neurovascular coupling in rat cerebral cortex

Kazuto Masamoto,[1] Mitsuhiro Fukuda,[1] Alberto Vazquez[1] and Seong-Gi Kim[1,2]
[1]Department of Radiology, University of Pittsburgh, 3025 East Carson Street, Pittsburgh, PA 15203, USA
[2]Department of Neurobiology, University of Pittsburgh, Pittsburgh, PA, USA

Keywords: fMRI, hemodynamic response function, laser-Doppler flowmetry, local field potential, somatosensory cortex

Abstract

Neurovascular coupling studies are widely conducted in anesthetized animals using functional magnetic resonance imaging (fMRI). In this study, the dose-dependent effects of isoflurane on neurovascular coupling were examined with concurrent recordings of the local field potential (FP) and cerebral blood flow (CBF) in the rat somatosensory cortex. Electrical forepaw stimulation was used, and consisted of either a single pulse or 10 pulses at various frequencies. We observed that the FP response to single-pulse stimulation remained unaffected across the different levels of isoflurane tested (1.1–2.1%), whereas the CBF response to single-pulse stimulation increased dose-dependently (7 ± 3% to 17 ± 4%). The isoflurane dose did not affect the vascular reactivity induced by a hypercapnic challenge. These findings suggest that the action of isoflurane affects the neurovascular mechanisms. For 10-pulse stimulation, the summation of the evoked FP responses monotonically decreased with an increase in the isoflurane dose, possibly due to enhancement of the neural adaptation. In contrast, the dose-dependent effect on the CBF response varied with the stimulus frequency; a dose-dependent decrease in the CBF response was observed for high-frequency stimulation, whereas a dose-dependent increase was observed for low-frequency stimulation. Furthermore, a linear time-invariant model consisting of the single-pulse hemodynamic impulse response convoluted with 10-pulse FP recordings showed that the neurovascular transfer function was altered by the isoflurane dose for high-frequency stimulation. These results indicate that careful and consistent maintenance of the depth of anesthesia is required when comparing fMRI data obtained from different animals or physiological and pharmacological manipulations.

Introduction

Functional magnetic resonance imaging (fMRI) measures brain activity via the changes in oxygen metabolism and hemodynamics that are associated with neural activity (i.e. neurometabolic and neurovascular couplings). However, the neural basis of the fMRI signal is still a subject of controversy (Mukamel *et al.*, 2005; Raichle & Mintun, 2006; Viswanathan & Freeman, 2007; Nir *et al.*, 2008). It has been shown that the fMRI signal correlates better with local field potential (FP) activity than with local spiking activity (Logothetis *et al.*, 2001; Nir *et al.*, 2007; Rauch *et al.*, 2008). Direct recordings of neural activity and hemodynamic signals from anesthetized rodents have been obtained to determine the relationships between these signals. In these studies, a linear relationship was observed between the integrated FP activity and hemodynamic signals induced by varying the strength or frequency of a sensory stimulus (Ngai *et al.*, 1999; Matsuura & Kanno, 2001; Sheth *et al.*, 2003), but a nonlinear relationship has also been reported (Nielsen & Lauritzen, 2001; Devor *et al.*, 2003; Sheth *et al.*, 2004; Hewson-Stoate *et al.*, 2005). However, these experiments were conducted under various types of anesthesia (e.g. α-chloralose, enflurane, and urethane), which makes it difficult to compare the results.

The depth of anesthesia can also modulate the neurovascular relationships through actions on the neural response, vascular reactivity, and/or neurovascular transfer mechanisms. Austin *et al.* (2005) showed that fMRI responses to somatosensory stimulation were unaffected by halothane anesthesia within a range of 0.7–1.5%, whereas Schulte & Hudetz (2006) showed that changes in cerebral blood flow (CBF) induced by visual stimulation were dose-dependently attenuated by halothane anesthesia over a range of 0.4–1.4%. Although these studies reported conflicting effects of anesthetic dose, the effects of anesthetic dose on neural activity were not directly compared. In our previous study, the neurovascular coupling properties were tested in the rat somatosensory cortex under 1.3% isoflurane, and a nonlinear relationship was found, depending on the stimulus pulse width, current, and frequency (Masamoto *et al.*, 2007). As a result of that report, questions arose of whether the observed neurovascular properties at 1.3% isoflurane could be generalized over different levels of isoflurane anesthesia.

In the present study, we aimed to determine the dose-dependent effects of isoflurane anesthesia on neurovascular coupling in the rat somatosensory cortex. By manipulation of the end-tidal concentrations of isoflurane (between 1.1 and 2.1%), the isoflurane dose effects on

Correspondence: Dr Seong-Gi Kim, [1]Department of Radiology, as above.
E-mail: kimsg@pitt.edu

Received 4 February 2009, revised 15 May 2009, accepted 20 May 2009

neural activity, vascular reactivity and hemodynamic responses were examined. First, the dose-dependent effect on vascular reactivity was assessed by measuring the change in CBF induced by a hypercapnic challenge, independently of neural activity. Second, using single-pulse stimulation, neural and hemodynamic impulse responses (HIRs) were determined, providing an 'intrinsic' neurovascular transfer function. Third, neurovascular responses to 10-pulse stimuli were also measured with variable stimulus frequencies. Finally, to generalize the neurovascular transfer function, apparent HIRs were calculated for each isoflurane dose condition and compared with the single-pulse HIR to examine isoflurane dose effects on neurovascular transfer mechanisms.

Materials and methods

Animal preparation

Animal use was in accordance with the standards for humane animal care and use as set by the Animal Welfare Act and the NIH Guide *Care and Use of Laboratory Animals*, and the experimental protocol used was approved by the University of Pittsburgh Institutional Animal Care and Use Committee. A total of twelve male Sprague–Dawley rats (350–470 g; Charles River Laboratories, Wilmington, MA, USA) were used for the single-pulse, impulse response study ($n = 6$), and the 10-pulse, frequency-dependent study ($n = 6$).

The animals were initially anesthetized with isoflurane (5% for induction, and 1.5–2% during surgery) in a mixture of oxygen (35–50%) and nitrous oxide (65–50%). Tracheal intubation was performed, and a catheter was placed into the femoral artery. A 5 × 7 mm portion of the left skull, centered 3.5 mm laterally and 0.5 mm rostrally from bregma, was thinned. After completion of the animal preparation, the inspired gas was converted to a mixture of air and pure oxygen (30–35% total oxygen) and the end-tidal concentration of isoflurane was adjusted to 1.3 ± 0.1% (∼1 minimum alveolar concentration) (Antognini *et al.*, 1999). Nitrous oxide, which was beneficial for stabilizing the depth of anesthesia for surgery, was replaced by air after surgery in all experiments to eliminate possible confounding effects. Preliminary data obtained showed that the evoked FP was greatly reduced when the animal was anesthetized with a mixture of isoflurane and nitrous oxide. End-tidal gas levels were monitored throughout the experiments with a multiparameter airway gas monitor (ULT-I, CAPNOMAC ULTIMA; Datex-Ohmeda, Inc., Madison, WI, USA), and the minute ventilation and respiratory rates were adjusted as needed. The physiological parameters, that is, fraction of inspiratory oxygen, end-tidal carbon dioxide, isoflurane concentration, arterial blood pressure, and electrocardiogram, were all recorded using polygraph data-acquisition software (ACK100W AcqKnowledge software; BIOPAC Systems, Inc., Goleta, CA, USA). The rectal temperature was maintained at 37 °C with a DC temperature control module. Arterial blood gas was sampled every 0.5–1.5 h and maintained within normal physiological limits (P_aO_2 = 104 ± 5 mmHg, P_aCO_2 = 36.4 ± 1.2 mmHg, pH = 7.491 ± 0.012 [mean ± standard deviation (SD)], 12 animals).

Isoflurane dose

The end-tidal isoflurane level was adjusted to be between 1.1 ± 0.1%, which minimally immobilizes the animals (i.e. low dosage), and 2.1 ± 0.1%, which is deep enough for surgery (i.e. high dosage). Two to five doses were tested over a range of 1.1–2.1% isoflurane in each animal. Whenever the isoflurane dose was adjusted, the spontaneous FP activity was monitored to determine when a steady state was reached. We observed that the pattern of spontaneous FP activity changed shortly after the changes in isoflurane dose (< 5 min) and stabilized within 10–15 min. Therefore, the experiments were initiated 15 min after the adjustment of the isoflurane dose. This criterion is supported by previous reports showing that the isoflurane concentration in arterial blood and brain tissue equilibrates after approximately 15 min (Lin, 1994; Antognini *et al.*, 1999). To minimize possible time-dependent effects, the experimental order of the various isoflurane doses was randomized and the experiments were completed within 4 h from the beginning of the first recording in each animal. Preliminary experiments showed that the relative laser-Doppler flowmetry (LDF) baseline change between the beginning of the final session (set to 1.1% isoflurane) and the beginning of the first session (set to 1.1% isoflurane) was 104 ± 13% over a time period of 184 ± 13 min ($n = 5$). This shift in the baseline LDF level could be due to the slow clearance of isoflurane from fat tissue, but the effect was not consistent (for example, LDF increased and decreased among subjects).

Hypercapnic challenge

Vascular reactivity was tested using a hypercapnic challenge performed in four of the six animals from the single-pulse experiment. A breathing mixture of 5% carbon dioxide and 95% air was administered while the end-tidal concentration of carbon dioxide and the CBF level were measured every 3 s from the onset of gas administration for up to 5 min. For this experiment, the baseline inspired gas mixture consisted of only air (without supplementary oxygen) to minimize potential influences of changes in the inspired oxygen fraction. To evaluate the vascular reactivity, the relative change in CBF was plotted against the end-tidal carbon dioxide level for each isoflurane dose condition tested. A linear least-squares fit was performed on all of the data points to determine whether the vascular reactivity is affected by the isoflurane dose. The arterial blood gas level was also measured before and about 5 min after the onset of gas administration [P_aCO_2 = 37 ± 2 mmHg and P_aCO_2 = 47 ± 3 mmHg before and after gas administration, respectively (mean ± SD), four animals].

Forepaw stimulation

Two needle electrodes were inserted under the skin of the right forepaw between digits two and four for delivery of the electrical stimulus (Silva *et al.*, 1999). Electrical pulses were given using a pulse generator and isolator (Master 8 and ISO-Flex; AMPI, Israel). For the single-pulse experiments, one-pulse stimulation (1.0-ms width and 1.5-mA current amplitude) was repeatedly applied every 30 s. For each condition, 50–100 runs were repeated to improve the signal-to-noise ratio. For the frequency-dependent study, 10-pulse stimuli (1.0-ms width and 1.0-mA current amplitude) were applied with different onset-to-onset intervals (50–500 ms) and a 40-s interval between stimulation runs (i.e. train). Five onset-to-onset intervals (also referred to as interpulse intervals) were tested: 50, 75, 100, 200 and 500 ms, corresponding to frequencies of 20, 13, 10, 5 and 2 Hz, respectively. For each stimulus frequency condition, 6–10 runs were performed, and the order of stimulation frequency was randomized. A slightly higher stimulus current was used for the single-pulse experiment than for the 10-pulse study (1.5 mA vs. 1.0 mA), to improve the signal-to-noise ratio.

Concurrent recordings of FP and CBF

To localize the forepaw activation area prior to placing the FP electrode and LDF probe, optical imaging of intrinsic signals was

performed using an experimental paradigm and a custom-made imaging system as previously reported (Masamoto *et al.*, 2007). Cortical images (3.7 × 4.9 mm) were captured with a charge-coupled device camera (CS8310; Tokyo Electric Industry, Japan) and a 10-bit frame grabber board at a rate of 30 frames per second, while the cortical surface was illuminated with filtered light (620 ± 10 nm). Each 6-s recording run was divided into 1 s of pre-stimulation baseline, 3 s of stimulation (1.0-ms width and 1.2–1.5-mA current, applied at 3 Hz), and 2 s of post-stimulation baseline, repeated 20 times. Temporal averaging (15 consecutive frames; 0.5 s/image) and spatial binning (2 × 2 pixels) were performed during off-line analysis. The activation focus was then determined to be the largest decrease in light reflectance (i.e. an increase in light absorption) observed between 0.5 and 2.5 s after the onset of stimulation.

The FP and CBF were concurrently recorded at the activation focus with a tungsten microelectrode (< 1 MΩ; FHC, Inc., Bowdoinham, ME, USA) and LDF (PeriFlux 4001 Master System; Perimed, Sweden), respectively, as described previously (Masamoto *et al.*, 2007). The spread of the FP signals was reported to span between 250 μm and a few millimeters in the visual cortex (Kreiman *et al.*, 2006; Liu & Newsome, 2006; Katzner *et al.*, 2009). The tip of the microelectrode was placed at a depth of 0.5–0.6 mm from the cortical surface, while a needle-type LDF probe (0.45-mm tip diameter and 0.15-mm fiber separation; Probe 411; Perimed) was placed on the surface of the thinned skull preparation above the activation area. To minimize the invasiveness of the procedure around the recording area and reduce potential motion artifacts, the thinned skull preparation was used. The microelectrode was inserted through a small slit made on the thinned skull just above the activation focus according to the optical imaging map, and the dura was then punctured with the electrode. The stereotaxic frame and the holders for the FP electrode and LDF probe were fixed to the table to minimize motion. The distance between the LDF probe and the insertion site of the electrode at the cortical surface was about 0.5 mm. The FP and CBF data were recorded using the BIOPAC data-acquisition software at a frequency of 1 kHz.

Data analysis

The FP data were averaged across all stimulation runs for each stimulation condition. The mean amplitude of the evoked FP was reported as the difference between the positive and negative peaks observed 5–20 ms after stimulation onset (Masamoto *et al.*, 2007). For the 10-pulse experiments, the summation of the evoked FP (ΣFP) was also achieved by summing the amplitude (minimum to maximum) of all 10 evoked FPs. The CBF data were first down-sampled by temporal averaging of 100 consecutive sampling points (resulting in a 0.1-s temporal resolution), and then averaged across all runs in each stimulation condition. The CBF response was normalized by the pre-stimulation baseline (i.e. mean over 5 s before stimulation onset), and the peak amplitude was measured. The fluctuation of the baseline level was also determined by measuring the mean and SD of the resting condition data over a period of 1 min. To compare data across animals, ΣFP and peak CBF were normalized by their respective maxima in each animal. All of the measurements of the mean arterial blood pressure (MABP), LDF, evoked FP and CBF were compared with their corresponding isoflurane concentration using linear regression, and the correlation coefficient was calculated. The significance of the slope being different from zero was assessed, and the statistical significance of the values observed for low-dose and high-dose conditions were determined by paired Student's *t*-test between subjects. Data are presented as mean ± standard deviation (SD), unless otherwise specified.

Linear time-invariant model

Hemodynamic responses induced by 10-pulse stimulation can be described as a linear combination of 10 individual, time-invariant, single-pulse responses. To examine this property for each stimulation frequency tested, the apparent HIR was determined by deconvolution of the 10-pulse CBF data with the evoked FPs (considering the exact time of each FP), assuming that

$$\text{Measured CBF data} = \text{Apparent HIR} \otimes \text{Evoked FPs} \quad (1)$$

where ⊗ indicates the convolution function. To compare the single-pulse data obtained and increase the signal-to-noise ratio, the CBF responses and FPs (without normalization) were averaged across all animals under low-dose (1.1%) and high-dose (2.1%) conditions. The single-pulse and 10-pulse studies were conducted in different animal groups to achieve sufficient signal averaging for each experiment. Considering the variation in the FP amplitude between the two studies, the measured CBF response was normalized by the individual FP amplitude, such that the apparent HIR was represented by the CBF response per millivolt of FP amplitude. The apparent HIR was then compared across stimulation frequencies under the low-dose and high-dose conditions. The peak intensity and full width at half-maximum (FWHM) of the HIR were calculated.

Results

Figure 1 shows the dose-dependent effect of isoflurane on the spontaneous FP activity measured in the rat somatosensory cortex. Under high-dose conditions (> 1.7% isoflurane), burst-suppression activity was evident, which is consistent with a previous report (Golanov *et al.*, 1994). When the isoflurane dose was increased or decreased in a stepwise fashion, a similar pattern in the spontaneous FP activity was reproducibly observed. Increasing the dose of isoflurane caused the systemic blood pressure to decrease in a dose-dependent fashion. A statistically significant difference in the MABP was observed between the low-dose and high-dose conditions (t_{11} = 4.19, P = 0.0008; Fig. 2A). In contrast, the baseline CBF level measured by LDF showed no detectable changes between the low-dose and high-dose conditions (t_{11} = 0.38, P = 0.36; Fig. 2B). Also, the baseline fluctuation level in the LDF signal (1 SD) was ∼9% of the mean, irrespective of the isoflurane dose.

In the single-pulse experiment, similar evoked FP response amplitudes were observed irrespective of the dose of isoflurane (Fig. 3A). No significant differences in the amplitude of the positive peak (0.88 ± 0.23 vs. 0.83 ± 0.25 mV, t_5 = 1.45, P = 0.10) and the negative peak (−0.74 ± 0.15 vs. −0.71 ± 0.22 mV, t_5 = 0.47, P = 0.33) were found between the low-dose and high-dose conditions. In contrast, a higher CBF response was observed under the high-dose condition (Fig. 3B). A significant difference in the peak amplitude of the evoked CBF (7 ± 3% vs. 17 ± 4%, t_5 = 5.61, P = 0.0012) and in FWHM (1.7 ± 0.3 s vs. 4.1 ± 0.8 s, t_5 = 6.52, P = 0.0006) was observed between the low-dose and high-dose conditions. Population data (n = 6) consistently showed similar evoked FP amplitudes, irrespective of the isoflurane level (r_{15} = 0.024, P = 0.93, Fig. 3C), and a significant correlation was observed between the peak amplitude of the evoked CBF and the isoflurane level (r_{15} = 0.78, P = 0.0002, Fig. 3D). Consequently, no correlation was observed between the evoked FP and CBF responses measured across different isoflurane doses (r_{15} = 0.030, P = 0.91, Fig. 3E). Also, it was confirmed that this variation in the evoked CBF was not solely due to the changes in MABP (r_{15} = −0.35, P = 0.16, Fig. 3F).

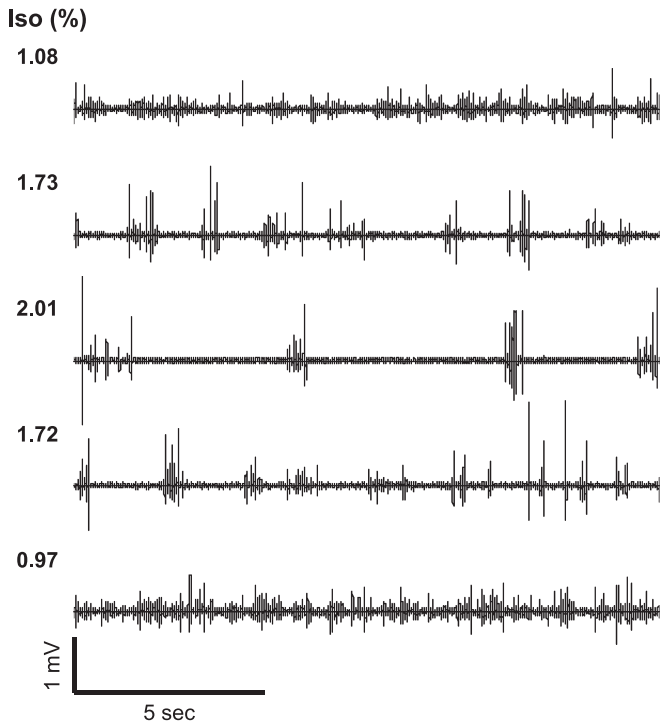

FIG. 1. Baseline spontaneous field potentials (FPs) induced by variable doses of isoflurane. In this representative animal, the isoflurane concentration (Iso) was changed from 1.1% (top) to 2.0% (middle) and again adjusted to 1.0% (bottom). In each condition, the spontaneous FP activity varied with the isoflurane dose, and a consistent pattern was reproducibly observed with the respective doses. Under high-dose conditions (= 1.7%), a burst-suppression pattern was evident. This pattern was consistently observed across all animals.

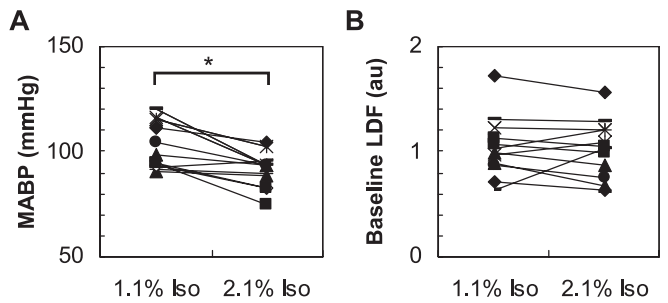

FIG. 2. Mean arterial blood pressure (MABP) band baseline blood flow level at variable doses of isoflurane. (A) Subject-to-subject comparison of MABP between low and high doses (n = 12). Note that the systemic blood pressure significantly decreased under high-dose conditions [2.1% isoflurane concentration (Iso)]. *P < 0.05. (B) Subject-to-subject comparison of the mean baseline laser-Doppler flowmetry (LDF) (n = 12). The baseline LDF level is presented as the raw LDF output value (au). No significant differences between low and high doses were observed.

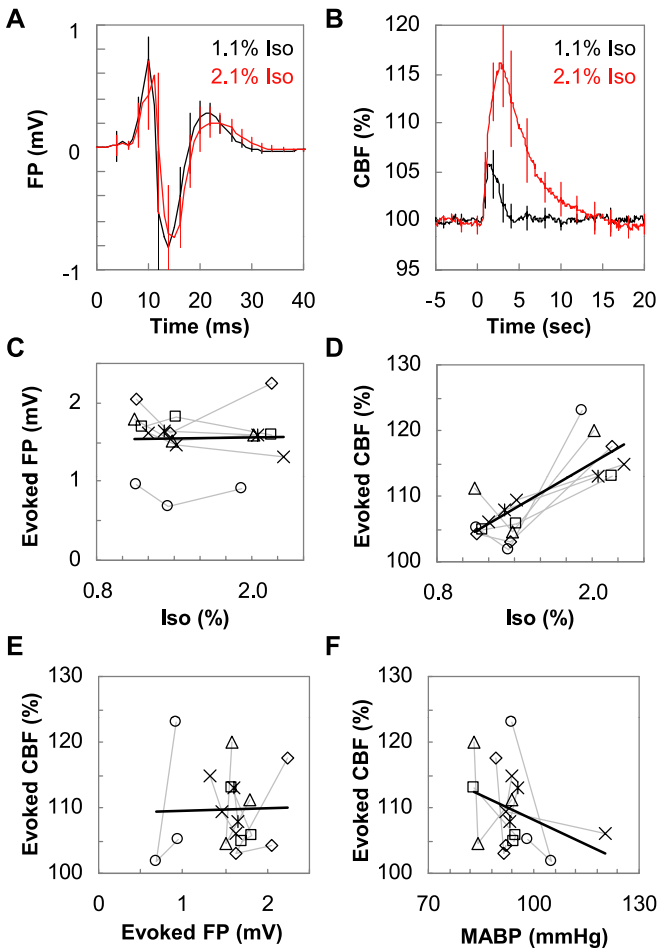

FIG. 3. Evoked field potential (FP) and blood flow response induced by single-pulse stimulation. (A) Averaged evoked FPs obtained from all six animals tested. The comparisons between low-dose (black) and high-dose (red) conditions showed that the amplitude of the evoked FP was relatively unaffected by the dose of isoflurane (Iso). One-pulse stimulation was given at time 0. Error bar: standard deviation (SD). (B) Averaged cerebral blood flow (CBF) time-course data obtained from the same six animals shown in A. The intensity of the CBF response was observed to increase at high isoflurane doses (red) as compared with low isoflurane doses (black). One-pulse stimulation was given at time 0. Error bar: SD. (C) Population data of evoked FP (n = 6). Each symbol represents individual animal data. The amplitude of the evoked FP was constant, irrespective of the level of isoflurane. No significant correlation between FP amplitude and isoflurane level was observed (r_{15} = 0.024, P = 0.93). (D) Population data of evoked CBF (n = 6). Identical symbols in C and D indicate data from the same animal. Note that the CBF response consistently increased in a dose-dependent manner (r_{15} = 0.78, P = 0.0002). (E) Scatter plot of evoked FP and evoked CBF. No clear correlation was observed between evoked FP and CBF across all data obtained from six animals obtained at different isoflurane levels (r_{15} = 0.030, P = 0.91). (F) Population data of evoked CBF vs. mean arterial blood pressure (MABP) (n = 6). There was no significant correlation between MABP and evoked CBF (r_{15} = −0.35, P = 0.16).

The dose-dependent increase in the CBF response could be due to a change in the vascular reactivity. To test this possibility, the CBF response to a hypercapnic challenge was measured. The results showed that there were no detectable differences in the CBF response (18 ± 6, 17 ± 4, and 18 ± 7; LDF perfusion unit per end-tidal level of carbon dioxide) among the tested levels of isoflurane (1.1, 1.4, and 2.1%, respectively; four animals).

In the 10-pulse experiment, the attenuation of the FP response was increased with increased isoflurane concentrations, and this was consistently observed across all stimulation conditions (Fig. 4A). At a given isoflurane level, a lower frequency stimulus (i.e. a longer interpulse interval) induced less attenuation in the 10-pulse-evoked FPs, and thus the larger ΣFP, as compared with higher-frequency stimulation (Fig. 4B). Population data (n = 6) showed a good linear correlation between the ΣFP and the isoflurane level, irrespective of the stimulus interval (or frequency) (r_{27} = −0.61, −0.89, −0.63, −0.78 and −0.66, and P = 0.0004, 0.0001, 0.0002, 0.0001 and

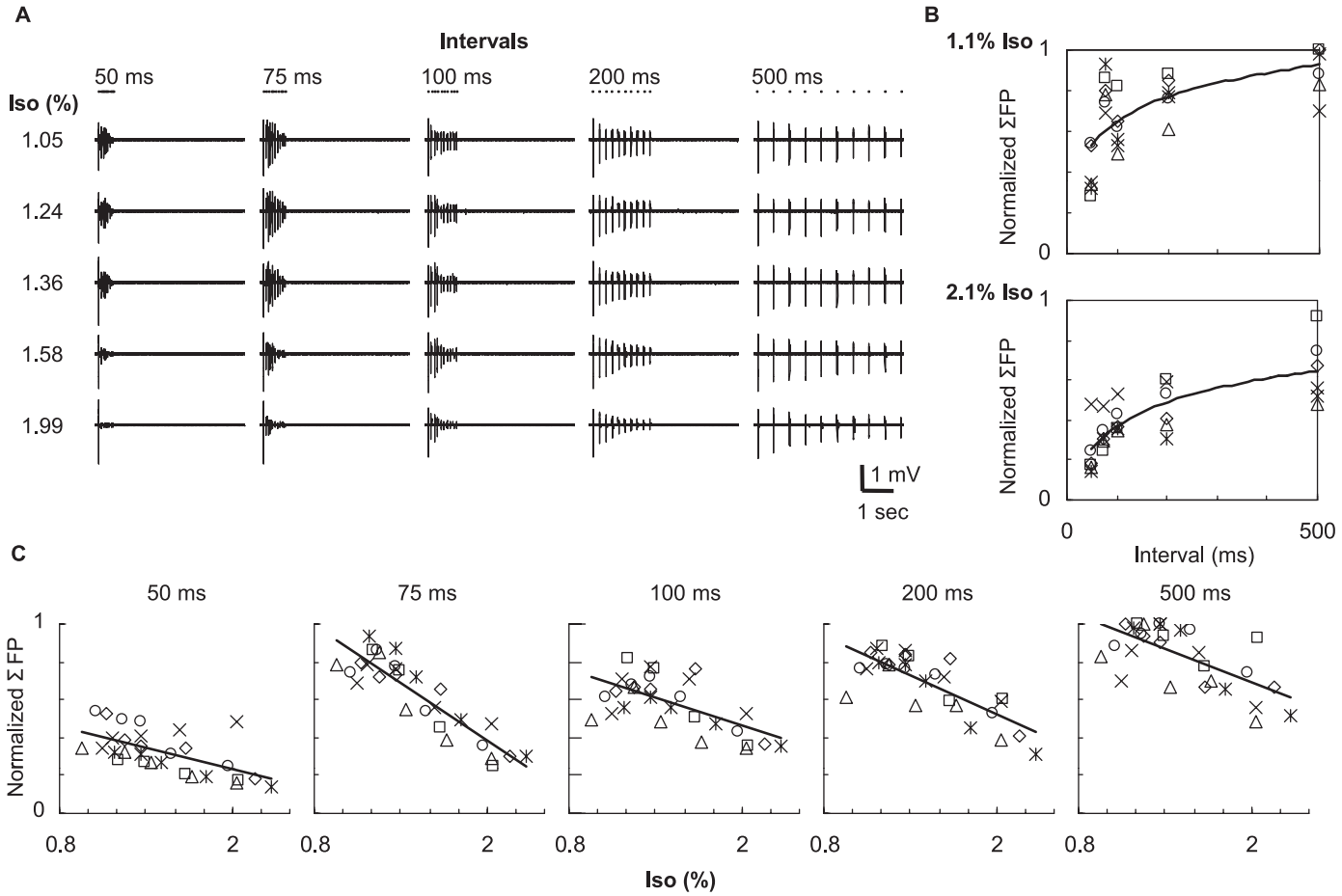

FIG. 4. Evoked field potentials (FPs) induced by 10-pulse stimuli. (A) Evoked FPs obtained from one representative animal. The attenuation of the FP response increased with isoflurane over all frequencies (interpulse intervals) tested. The dot shown above each FP trace indicates the onset time for each pulse; for each stimulus, 10 dots indicate the time for which the 10 pulses were delivered. (B) Population data (n = 6) of the ΣFP against interpulse interval at the same isoflurane level (Iso) (top, 1.1%; bottom, 2.1%). Each symbol represents data from individual animals normalized by the highest ΣFP in each animal. As expected, the lower-frequency stimuli (i.e. longer interpulse intervals) induced higher ΣFPs under low-dose and high-dose conditions. The curve fit was performed in logarithmic scale. (C) Population data (n = 6) of the ΣFP plotted against isoflurane level at the same stimulation frequency. With increasing doses of isoflurane, the evoked FPs were suppressed over all frequency conditions, and thus significant negative correlations between ΣFP and isoflurane level were observed.

0.0001, for 50-ms, 75-ms, 100-ms, 200-ms and 500-ms intervals, respectively).

If a time-invariant linear relationship (Eqn. 1) is valid for the relationship between the evoked FP and CBF response, it is expected that, like the ΣFP activity, the CBF response to 10-pulse stimuli will monotonically decrease with an increase in the dose of isoflurane. This case was found only for high-frequency stimulation (e.g. 50-ms and 75-ms intervals) (Fig. 5A). In contrast, a dose-dependent increase in the CBF response was observed for low-frequency stimulation (e.g. 200-ms and 500-ms intervals) (Fig. 5A). Hence, the frequency-dependent pattern of the CBF response differed between the low-dose and high-dose conditions (Fig. 5B). Population data (n = 6) clearly showed the dose-dependent effects of isoflurane on the CBF response as a function of the stimulus frequency (Fig. 5C). A negative and a positive correlation was observed, depending on the stimulus frequency: $r_{27} = -0.44$, -0.72, -0.03, 0.38 and 0.67, and $P = 0.017$, 0.0001, 0.90, 0.043 and 0.0001, for 50-ms, 75-ms, 100-ms, 200-ms and 500-ms intervals, respectively.

Finally, a comparison between the apparent HIR and the measured single-pulse HIR revealed that the neurovascular transfer function was altered by the isoflurane dose as a function of the stimulation frequency (Fig. 6A and B). Under high-dose conditions, the peak intensity of the apparent HIR monotonically decreased with increases in the stimulation frequency, and reached half the intensity of the single-pulse HIR for the 50-ms stimulation interval condition (10% for single-pulse HIR vs. 5–9% for apparent HIR; Fig. 6C). However, the width of the apparent HIR at this stimulation interval (50 ms) was found to be the same as the single-pulse HIR (4.6 s at FWHM). Under low-dose conditions, a slight decrease in the peak intensity of the apparent HIR was observed with decreasing stimulation frequencies (5–3%; Fig. 6C). A comparison between the apparent HIR and the single-pulse HIR showed reasonably good agreement in the peak intensity (4% for single-pulse HIR) and width (1.9 s for single-pulse HIR), except for the 75-ms interval data (4.0 s). The observed difference between model and data indicates that nonlinear components may act on the neurovascular transfer mechanism at this specific frequency.

Discussion

The present study shows that the neural impulse response as measured by local FP was independent of the dose of isoflurane

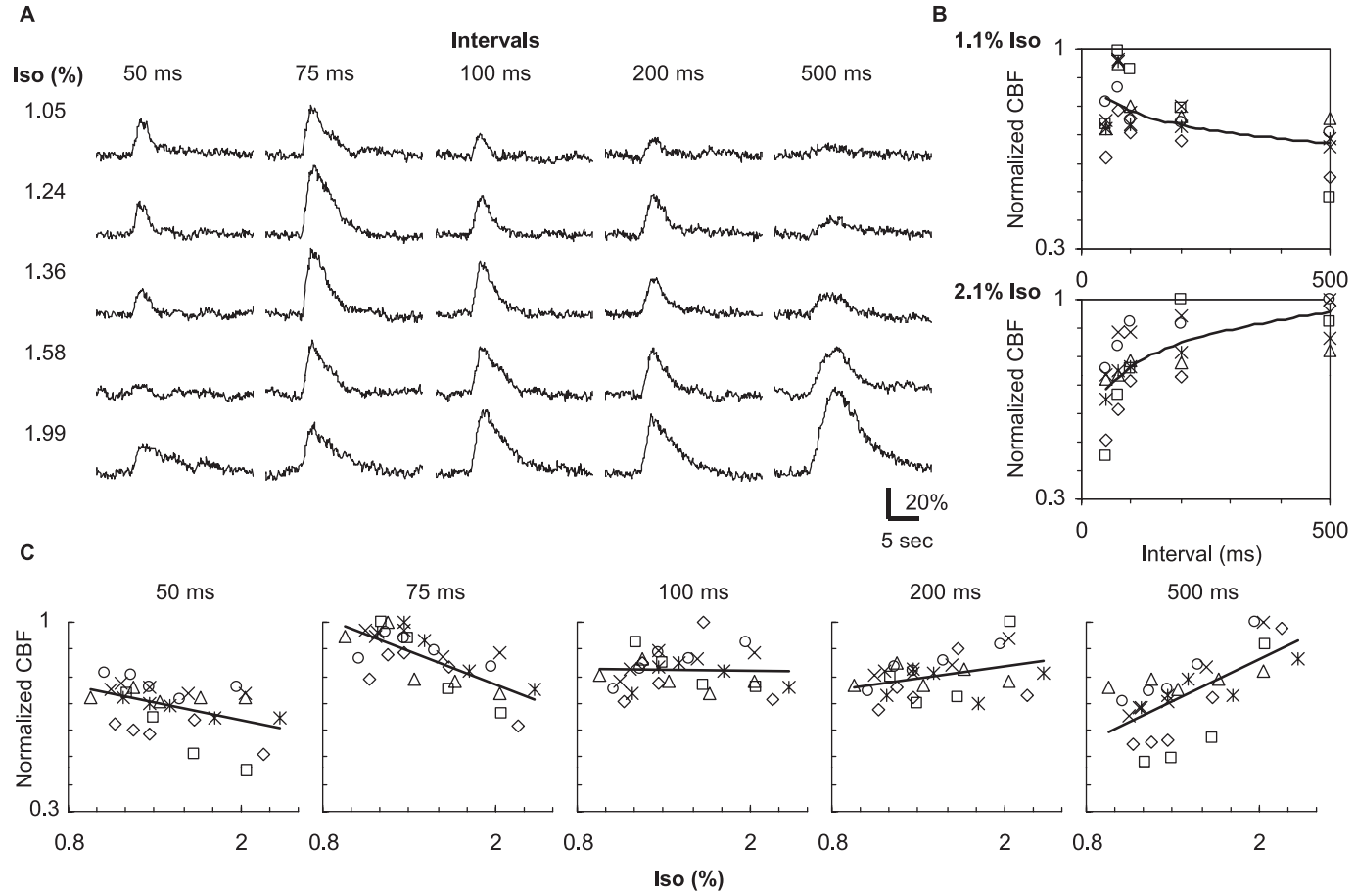

FIG. 5. Evoked blood flow response induced by 10-pulse stimuli. (A) Cerebral blood flow (CBF) data obtained from a representative animal. The intensity of the CBF response decreased for high-frequency stimuli (50-ms and 75-ms intervals) with increases in the isoflurane level (Iso), whereas the CBF response dose-dependently increased for low-frequency stimuli (200-ms and 500-ms intervals). Consequently, the effect of the isoflurane dose on the CBF response was opposite between low-frequency and high-frequency stimuli. (B) Population data (n = 6) of the CBF peak plotted against interpulse interval under low-dose and high-dose conditions. Each symbol represents the data from individual animals normalized by their corresponding peak. The frequency-dependent CBF response also varied as a function of the isoflurane level; higher-frequency stimuli (shorter intervals) induced larger CBF changes under low-dose conditions (top), whereas lower-frequency stimuli (longer intervals) induced larger CBF changes under high-dose conditions (bottom). The curve fit was performed in a logarithmic scale. (C) Population data (n = 6) of the CBF peak plotted against isoflurane level at the same stimulation frequency. The correlation between CBF peak and isoflurane level varied from negative to positive as a function of the interpulse interval.

administered (1.1–2.1%), whereas the HIR, measured by LDF, varied as a function of the isoflurane dose administered (Fig. 3). As relatively constant neural responses and vascular reactivities tested with a hypercapnic challenge were observed, these findings indicate that the action site of isoflurane directly participates in the neurovascular transfer mechanism. For the 10-pulse stimuli, the evoked ΣFP decreased dose-dependently over all of the frequency conditions tested, due to a dose-dependent newal adaptation effect (Fig. 4). However, the CBF response showed either a dose-dependent decrease or a dose-dependent increase, depending on the stimulus frequency (Fig. 5). Specifically, the dose-dependent effect was opposite between low-frequency and high-frequency stimuli, which may indicate divergent effects of the anesthetic dose on the activity-induced hemodynamic responses (Hyder *et al.*, 2002; Austin *et al.*, 2005; Schulte & Hudetz, 2006). Furthermore, the dose-dependent effect on the evoked CBF was found to be different from that on the evoked FP responses (Figs 4 and 5). These findings show that careful monitoring of the depth of anesthesia and consistent use of the stimulus paradigm are necessary for accurate interpretation and reliable comparisons of hemodynamic-based functional studies (e.g. fMRI), both within and between anesthetized subjects.

Impact of isoflurane dose on neurovascular transfer mechanisms

Isoflurane is widely used for physiological studies, because it provides a stable condition, allows easy control of the targeted depth of anesthesia, and can be used repeatedly for survival experiments in the same animal (Lukasik & Gillies, 2003; Masamoto *et al.*, 2007). In addition, the action of isoflurane is relatively well studied in comparison with those of other, more conventional, injectable anesthetics [for a review, see Campagna *et al.* (2003)]. It has been shown that isoflurane acts at intracortical sites and directly depresses cortical activity (Hentschke *et al.*, 2005). Previous studies have consistently shown that isoflurane dose-dependently depresses excitatory transmission through inhibition of glutamate release (Haseneder *et al.*, 2004; Sandstrom, 2004; Wu *et al.*, 2004). At the same time, isoflurane is thought to affect ligand-gated ion channels, inhibiting

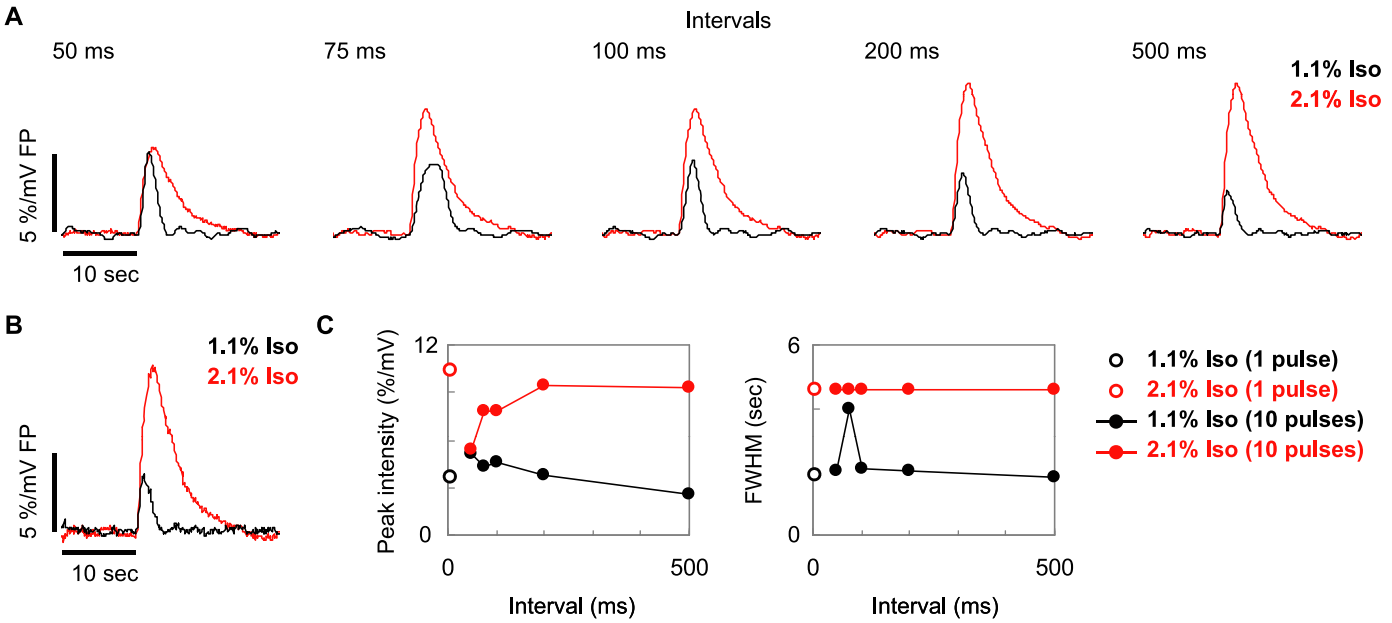

FIG. 6. Comparison of the apparent hemodynamic impulse responses determined using a linear time-invariant model. (A) The apparent hemodynamic impulse response (HIR) calculated from field potential (FP) and cerebral blood flow data obtained from 10-pulse experiments. (B) The single-pulse HIR. The peak intensity was corrected by the measured FP amplitude. As compared with measured single-pulse HIR (B), the apparent HIR (A) was changed, especially for high-frequency stimuli (< 200-ms intervals) for both low-dose (black) and high-dose (red) conditions. (C) Peak intensity and full width at half-maximum (FWHM) of the respective HIRs. For low-frequency stimulation (= 200-ms intervals), a similar peak intensity was observed between the apparent HIR (closed circle) and the single-pulse HIR (open circle), indicating a good prediction by a linear time-invariant system (Eqn. 1). Also, FWHM was observed to be in good agreement with that of single-pulse HIR, except for the 75-ms interval stimulation under low-dose conditions. Iso, isoflurane level.

N-methyl-D-aspartate receptors and potentiating γ-aminobutyric acid type A receptors (Ranft *et al.*, 2004; Hentschke *et al.*, 2005; Dickinson *et al.*, 2007; Kelly *et al.*, 2007). Furthermore, dose-dependent enhancement of glutamate uptake by astrocytes has been reported (Miyazaki *et al.*, 1997). Although no detectable changes in the single-pulse FP were observed in the present study (Fig. 3), these known actions of isoflurane may contribute to the dose-dependent change in the neurovascular transfer function. A recent study showed that some receptor functions that do not participate in the evoked FP components can affect the intensity of hemodynamic changes (Hoffmeyer *et al.*, 2007). Future studies are necessary to identify the exact site(s) of isoflurane action that would participate in the neurovascular transfer mechanism(s).

As isoflurane is also known to be a potent vasodilator (Flynn *et al.*, 1992; Farber *et al.*, 1997), it is likely that the dose of isoflurane affects the cerebrovascular reactivity. In our study, however, we did not observe consistent effects of isoflurane dose on the baseline CBF level measured with LDF, although dose-dependent decreases in the systemic blood pressure were observed (Fig. 2). One possible explanation is that the slow change in anesthetic dose may preserve the experimental condition within the autoregulatory adjustment regime of the local CBF (Schulte & Hudetz, 2006). As 15 min was allotted after the adjustment of the isoflurane dose prior to recording, there may have been sufficient time for autoregulation to adjust local blood flow. Supporting this notion, previous studies have consistently found that autoregulatory control is preserved under 0.7–2.8% isoflurane anesthesia (Hudetz *et al.*, 1994; Lee *et al.*, 1994). These studies performed with LDF measurements have also shown an anesthesia dose-dependent increase in the baseline CBF under either halothane (0.5–2.2%) or isoflurane (0.7–2.8%) anesthesia conditions (Hudetz *et al.*, 1994; Lee *et al.*, 1994). However, a later study from one of the groups found no dependencies of the halothane dose (0.4–1.4%) on the baseline CBF measured with LDF (Schulte & Hudetz, 2006), irrespective of constant maintenance of the systemic blood pressure. This discrepancy could be due to differences in the location and size of the LDF probe, physiological variability, and/or the experimental protocol used. A recent report also showed that isoflurane induced breakdown of the blood–brain barrier, accompanied by a local increase in CBF (Tétrault *et al.*, 2008). We did not observe detectable increases in the CBF baseline, suggesting that disruption of the blood–brain barrier was unlikely in our experimental conditions. In addition, we observed that the vascular reactivity tested with a hypercapnia challenge was similarly preserved (1.1–2.1% isoflurane), which is also consistent with previous reports (Hudetz *et al.*, 1994; Sicard *et al.*, 2003). In summary, the dose-dependent effect of isoflurane on the vascular physiology is not the major factor contributing to the dose-dependent effects on the HIR presented here.

Nonlinearity in stimulation frequency-dependent neurovascular responses

Some authors have proposed that the neurovascular transfer function can be explained by a linear time-invariant system (Boynton *et al.*, 1996; Dale & Buckner, 1997), which potentially provides a formula with which to compute neural activities from hemodynamic signals. However, later studies have shown that the neurovascular coupling has nonlinear components (Vazquez & Noll, 1998; Glover, 1999; Miller *et al.*, 2001; Devor *et al.*, 2003; Nemoto *et al.*, 2004; Martindale *et al.*, 2005), and claimed that nonlinear relationships capture a wider range of neurovascular behaviors (Sheth *et al.*, 2004; Hewson-Stoate *et al.*, 2005). In the present study, the neurovascular relationship seen with variable stimulation frequencies was also altered by the dose of isoflurane (Figs 4 and 5). This finding can be explained by two major factors: (i) a dose-dependent effect of isoflurane on the neurovascular

transfer function; and (ii) a stimulus frequency-dependent nonlinear component. As our results obtained with a linear time-invariant model showed good correspondence between the measured single-pulse HIR and the apparent HIR in lower-frequency conditions for both low and high isoflurane doses (Fig. 6), our findings suggest that isoflurane action further contributes to frequency-dependent nonlinear behavior under higher-frequency stimulation. The frequency-dependent mechanism of the neurovascular transfer function was actually shown by a recent study demonstrating that the NMDA receptor activity only contributes to the CBF response for high-frequency stimulation (> 7 Hz) (Hoffmeyer *et al.*, 2007). Furthermore, a comparison of the neurovascular couplings in anesthetized and alert animals is essential to extend our findings to human studies. There have been several reports on the differences in magnitude and localization of the hemodynamic-based neuroimaging signals in anesthetized vs. awake states (Lahti *et al.*, 1999; Shtoyerman *et al.*, 2000; Peeters *et al.*, 2001; Berwick *et al.*, 2002; Martin *et al.*, 2002, 2006; Sachdev *et al.*, 2003; Sicard *et al.*, 2003; Chen *et al.*, 2005; Fukuda *et al.*, 2005; Zhao *et al.*, 2007). These state-dependent variations could be explained by direct interference of the anesthetic action not only in cortical excitability, but also in the neurovascular transfer mechanisms at intracortical sites where the imaging signals were obtained.

Acknowledgements

This study was supported by the National Institutes of Health (EB003375, EB003324, and NS044589). We thank Ms Michelle Tasker for assisting in animal preparation.

Abbreviations

CBF, cerebral blood flow; fMRI, functional magnetic resonance imaging; FP, field potential; FWHM, full width at half-maximum; HIR, hemodynamic impulse response; LDF, laser-Doppler flowmetry; MABP, mean arterial blood pressure; SD, standard deviation.

References

Antognini, J.F., Wang, X.W. & Carstens, E. (1999) Quantitative and qualitative effects of isoflurane on movement occurring after noxious stimulation. *Anesthesiology*, **91**, 1064–1071.

Austin, V.C., Blamire, A.M., Allers, K.A., Sharp, T., Styles, P., Matthews, P.M. & Sibson, N.R. (2005) Confounding effects of anesthesia on functional activation in rodent brain: a study of halothane and alpha-chloralose anesthesia. *Neuroimage*, **24**, 92–100.

Berwick, J., Martin, C., Martindale, J., Jones, M., Johnston, D., Zheng, Y., Redgrave, P. & Mayhew, J. (2002) Hemodynamic response in the unanesthetized rat: intrinsic optical imaging and spectroscopy of the barrel cortex. *J. Cereb. Blood Flow Metab.*, **22**, 670–679.

Boynton, G.M., Engel, S.A., Glover, G.H. & Heeger, D.J. (1996) Linear systems analysis of functional magnetic resonance imaging in human V1. *J. Neurosci.*, **16**, 4207–4221.

Campagna, J.A., Miller, K.W. & Forman, S.A. (2003) Mechanisms of actions of inhaled anesthetics. *N. Engl. J. Med.*, **348**, 2110–2124.

Chen, L.M., Friedman, R.M. & Roe, A.W. (2005) Optical imaging of SI topography in anesthetized and awake squirrel monkeys. *J. Neurosci.*, **25**, 7648–7659.

Dale, A.M. & Buckner, R.L. (1997) Selective averaging of rapidly presented individual trials using fMRI. *Hum. Brain Mapp.*, **5**, 329–340.

Devor, A., Dunn, A.K., Andermann, M.L., Ulbert, I., Boas, D.A. & Dale, A.M. (2003) Coupling of total hemoglobin concentration, oxygenation, and neural activity in rat somatosensory cortex. *Neuron*, **39**, 353–359.

Dickinson, R., Peterson, B.K., Banks, P., Simillis, C., Martin, J.C., Valenzuela, C.A., Maze, M. & Franks, N.P. (2007) Competitive inhibition at the glycine site of the N-methyl-D-aspartate receptor by the anesthetics xenon and isoflurane: evidence from molecular modeling and electrophysiology. *Anesthesiology*, **107**, 756–767.

Farber, N.E., Harkin, C.P., Niedfeldt, J., Hudetz, A.G., Kampine, J.P. & Schmeling, W.T. (1997) Region-specific and agent-specific dilation of intracerebral microvessels by volatile anesthetics in rat brain slices. *Anesthesiology*, **87**, 1191–1198.

Flynn, N.M., Buljubasic, N., Bosnjak, Z.J. & Kampine, J.P. (1992) Isoflurane produces endothelium-independent relaxation in canine middle cerebral arteries. *Anesthesiology*, **76**, 461–467.

Fukuda, M., Rajagopalan, U.M., Homma, R., Matsumoto, M., Nishizaki, M. & Tanifuji, M. (2005) Localization of activity-dependent changes in blood volume to submillimeter-scale functional domains in cat visual cortex. *Cereb. Cortex*, **15**, 823–833.

Glover, G.H. (1999) Deconvolution of impulse response in event-related BOLD fMRI. *Neuroimage*, **9**, 416–429.

Golanov, E.V., Yamamoto, S. & Reis, D.J. (1994) Spontaneous waves of cerebral blood flow associated with a pattern of electrocortical activity. *Am. J. Physiol.*, **266**, R204–R214.

Haseneder, R., Kurz, J., Dodt, H.U., Kochs, E., Zieglgänsberger, W., Scheller, M., Rammes, G. & Hapfelmeier, G. (2004) Isoflurane reduces glutamatergic transmission in neurons in the spinal cord superficial dorsal horn: evidence for a presynaptic site of an analgesic action. *Anesth. Analg.*, **98**, 1718–1723.

Hentschke, H., Schwarz, C. & Antkowiak, B. (2005) Neocortex is the major target of sedative concentrations of volatile anaesthetics: strong depression of firing rates and increase of GABAA receptor-mediated inhibition. *Eur. J. Neurosci.*, **21**, 93–102.

Hewson-Stoate, N., Jones, M., Martindale, J., Berwick, J. & Mayhew, J. (2005) Further nonlinearities in neurovascular coupling in rodent barrel cortex. *Neuroimage*, **24**, 565–574.

Hoffmeyer, H.W., Enager, P., Thomsen, K.J. & Lauritzen, M.J. (2007) Nonlinear neurovascular coupling in rat sensory cortex by activation of transcallosal fibers. *J. Cereb. Blood Flow Metab.*, **27**, 575–587.

Hudetz, A.G., Lee, J.G., Smith, J.J., Bosnjak, Z.J. & Kampine, J.P. (1994) Effects of volatile anesthetics on cerebrocortical laser Doppler flow: hyperemia, autoregulation, carbon dioxide response, flow oscillations, and role of nitric oxide. *Adv. Pharmacol.*, **31**, 577–593.

Hyder, F., Rothman, D.L. & Shulman, R.G. (2002) Total neuroenergetics support localized brain activity: implications for the interpretation of fMRI. *Proc. Natl Acad. Sci. USA*, **99**, 10771–10776.

Katzner, S., Nauhaus, I., Benucci, A., Bonin, V., Ringach, D.L. & Carandini, M. (2009) Local origin of field potentials in visual cortex. *Neuron*, **61**, 35–41.

Kelly, E.W., Solt, K. & Raines, D.E. (2007) Volatile aromatic anesthetics variably impact human gamma-aminobutyric acid type A receptor function. *Anesth. Analg.*, **105**, 1287–1292.

Kreiman, G., Hung, C.P., Kraskov, A., Quiroga, R.Q., Poggio, T. & DiCarlo, J.J. (2006) Object selectivity of local field potentials and spikes in the macaque inferior temporal cortex. *Neuron*, **49**, 433–445.

Lahti, K.M., Ferris, C.F., Li, F., Sotak, C.H. & King, J.A. (1999) Comparison of evoked cortical activity in conscious and propofol-anesthetized rats using functional MRI. *Magn. Reson. Med.*, **41**, 412–416.

Lee, J.G., Hudetz, A.G., Smith, J.J., Hillard, C.J., Bosnjak, Z.J. & Kampine, J.P. (1994) The effects of halothane and isoflurane on cerebrocortical microcirculation and autoregulation as assessed by laser-Doppler flowmetry. *Anesth. Analg.*, **79**, 58–65.

Lin, C.Y. (1994) Uptake of anaesthetic gases and vapours. *Anaesth. Intensive Care*, **22**, 363–373.

Liu, J. & Newsome, W.T. (2006) Local field potential in cortical area MT: stimulus tuning and behavioral correlations. *J. Neurosci.*, **26**, 7779–7790.

Logothetis, N.K., Pauls, J., Augath, M., Trinath, T. & Oeltermann, A. (2001) Neurophysiological investigation of the basis of the fMRI signal. *Nature*, **412**, 150–157.

Lukasik, V.M. & Gillies, R.J. (2003) Animal anaesthesia for in vivo magnetic resonance. *NMR Biomed.*, **16**, 459–467.

Martin, C., Berwick, J., Johnston, D., Zheng, Y., Martindale, J., Port, M., Redgrave, P. & Mayhew, J. (2002) Optical imaging spectroscopy in the unanaesthetised rat. *J. Neurosci. Methods*, **120**, 25–34.

Martin, C., Martindale, J., Berwick, J. & Mayhew, J. (2006) Investigating neural–hemodynamic coupling and the hemodynamic response function in the awake rat. *NeuroImage*, **32**, 33–48.

Martindale, J., Berwick, J., Martin, C., Kong, Y., Zheng, Y. & Mayhew, J. (2005) Long duration stimuli and nonlinearities in the neural–haemodynamic coupling. *J. Cereb. Blood Flow Metab.*, **25**, 651–661.

Masamoto, K., Kim, T., Fukuda, M., Wang, P. & Kim, S.G. (2007) Relationship between neural, vascular, and BOLD signals in isoflurane-anesthetized rat somatosensory cortex. *Cereb. Cortex*, **17**, 942–950.

Matsuura, T. & Kanno, I. (2001) Quantitative and temporal relationship between local cerebral blood flow and neuronal activation induced by somatosensory stimulation in rats. *Neurosci. Res.*, **40**, 281–290.
Miller, K.L., Luh, W.M., Liu, T.T., Martinez, A., Obata, T., Wong, E.C., Frank, L.R. & Buxton, R.B. (2001) Nonlinear temporal dynamics of the cerebral blood flow response. *Hum. Brain Mapp.*, **13**, 1–12.
Miyazaki, H., Nakamura, Y., Arai, T. & Kataoka, K. (1997) Increase of glutamate uptake in astrocytes: a possible mechanism of action of volatile anesthetics. *Anesthesiology*, **86**, 1359–1366.
Mukamel, R., Gelbard, H., Arieli, A., Hasson, U., Fried, I. & Malach, R. (2005) Coupling between neuronal firing, field potentials, and FMRI in human auditory cortex. *Science*, **309**, 951–954.
Nemoto, M., Sheth, S., Guiou, M., Pouratian, N., Chen, J.W. & Toga, A.W. (2004) Functional signal- and paradigm-dependent linear relationships between synaptic activity and hemodynamic responses in rat somatosensory cortex. *J. Neurosci.*, **24**, 3850–3861.
Ngai, A.C., Jolley, M.A., D'Ambrosio, R., Meno, J.R. & Winn, H.R. (1999) Frequency-dependent changes in cerebral blood flow and evoked potentials during somatosensory stimulation in the rat. *Brain Res.*, **837**, 221–228.
Nielsen, A. & Lauritzen, M. (2001) Coupling and uncoupling of activity-dependent increases of neuronal activity and blood flow in rat somatosensory cortex. *J. Physiol.*, **533**, 773–785.
Nir, Y., Fisch, L., Mukamel, R., Gelbard-Sagiv, H., Arieli, A., Fried, I. & Malach, R. (2007) Coupling between neuronal firing rate, gamma LFP, and BOLD fMRI is related to interneuronal correlations. *Curr. Biol.*, **17**, 1275–1285.
Nir, Y., Dinstein, I., Malach, R. & Heeger, D.J. (2008) BOLD and spiking activity. *Nat. Neurosci.*, **11**, 523–524.
Peeters, R.R., Tindemans, I., De Schutter, E. & Van der Linden, A. (2001) Comparing BOLD fMRI signal changes in the awake and anesthetized rat during electrical forepaw stimulation. *Magn. Reson. Imaging*, **19**, 821–826.
Raichle, M.E. & Mintun, M.A. (2006) Brain work and brain imaging. *Annu. Rev. Neurosci.*, **29**, 449–476.
Ranft, A., Kurz, J., Deuringer, M., Haseneder, R., Dodt, H.U., Zieglgänsberger, W., Kochs, E., Eder, M. & Hapfelmeier, G. (2004) Isoflurane modulates glutamatergic and GABAergic neurotransmission in the amygdala. *Eur. J. Neurosci.*, **20**, 1276–1280.
Rauch, A., Rainer, G. & Logothetis, N.K. (2008) The effect of a serotonin-induced dissociation between spiking and perisynaptic activity on BOLD functional MRI. *Proc. Natl Acad. Sci. USA*, **105**, 6759–6764.
Sachdev, R.N., Champney, G.C., Lee, H., Price, R.R., Pickens, D.R. III, Morgan, V.L., Stefansic, J.D., Melzer, P. & Ebner, F.F. (2003) Experimental model for functional magnetic resonance imaging of somatic sensory cortex in the unanesthetized rat. *Neuroimage*, **19**, 742–750.
Sandstrom, D.J. (2004) Isoflurane depresses glutamate release by reducing neuronal excitability at the Drosophila neuromuscular junction. *J. Physiol.*, **558**, 489–502.
Schulte, M.L. & Hudetz, A.G. (2006) Functional hyperemic response in the rat visual cortex under halothane anesthesia. *Neurosci. Lett.*, **394**, 63–68.
Sheth, S., Nemoto, M., Guiou, M., Walker, M., Pouratian, N. & Toga, A.W. (2003) Evaluation of coupling between optical intrinsic signals and neuronal activity in rat somatosensory cortex. *Neuroimage*, **19**, 884–894.
Sheth, S.A., Nemoto, M., Guiou, M., Walker, M., Pouratian, N. & Toga, A.W. (2004) Linear and nonlinear relationships between neuronal activity, oxygen metabolism, and hemodynamic responses. *Neuron*, **42**, 347–355.
Shtoyerman, E., Arieli, A., Slovin, H., Vanzetta, I. & Grinvald, A. (2000) Long-term optical imaging and spectroscopy reveal mechanisms underlying the intrinsic signal and stability of cortical maps in V1 of behaving monkeys. *J. Neurosci.*, **20**, 8111–8121.
Sicard, K., Shen, Q., Brevard, M.E., Sullivan, R., Ferris, C.F., King, J.A. & Duong, T.Q. (2003) Regional cerebral blood flow and BOLD responses in conscious and anesthetized rats under basal and hypercapnic conditions: implications for functional MRI studies. *J. Cereb. Blood Flow Metab.*, **23**, 472–481.
Silva, A.C., Lee, S.P., Yang, G., Iadecola, C. & Kim, S.G. (1999) Simultaneous blood oxygenation level-dependent and cerebral blood flow functional magnetic resonance imaging during forepaw stimulation in the rat. *J. Cereb. Blood Flow Metab.*, **19**, 871–879.
Tétrault, S., Chever, O., Sik, A. & Amzica, F. (2008) Opening of the blood–brain barrier during isoflurane anaesthesia. *Eur. J. Neurosci.*, **28**, 1330–1341.
Vazquez, A.L. & Noll, D.C. (1998) Nonlinear aspects of the BOLD response in functional MRI. *Neuroimage*, **7**, 108–118.
Viswanathan, A. & Freeman, R.D. (2007) Neurometabolic coupling in cerebral cortex reflects synaptic more than spiking activity. *Nat. Neurosci.*, **10**, 1308–1312.
Wu, X.S., Sun, J.Y., Evers, A.S., Crowder, M. & Wu, L.G. (2004) Isoflurane inhibits transmitter release and the presynaptic action potential. *Anesthesiology*, **100**, 663–670.
Zhao, F., Jin, T., Wang, P. & Kim, S.G. (2007) Isoflurane anesthesia effect in functional imaging studies. *Neuroimage*, **38**, 3–4.